**Supplemental Information**

# Hydrothermal Temperature Driven Evolution of Morphology and Electrocatalytic Properties of Hierarchical Nanostructured CoFe-LDHs as Highly Efficient Electrocatalysts for Oxygen Evolution Reaction

Lin Tang, Xiaoli Jiang, Qiaoji Zheng*, Dunmin Lin

College of Chemistry and Materials Science, Sichuan Normal University, Chengdu 610066, China

**Figures:**

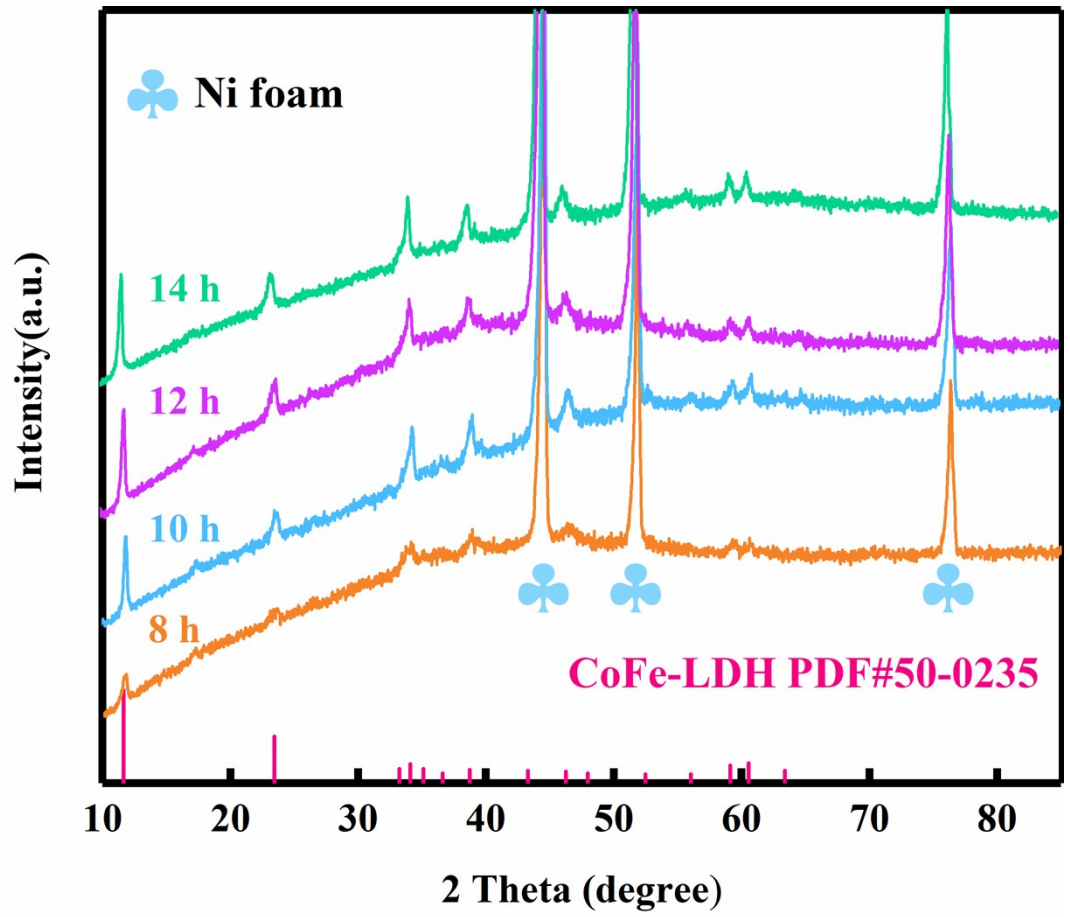


**Fig. S1** XRD patterns for CoFe-LDH-120 at different hydrothermal times.

* Corresponding author: Email: joyce@sicnu.edu.cn (Qiaoji Zheng); Fax: +86 28 84760802 Tel: +86 28 84760802

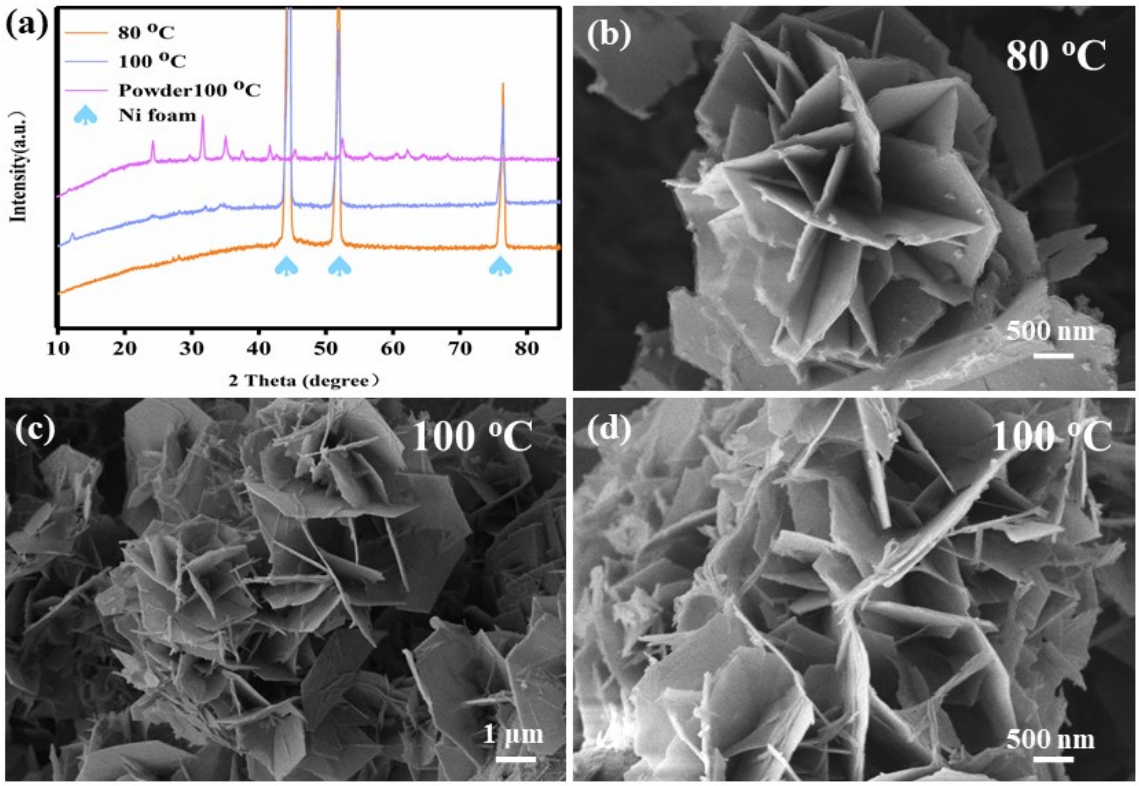


**Fig. S2** (a) XRD patterns for $Fe(OH)_3$ of different hydrothermal temperatures; SEM image of (b) $Fe(OH)_3$/NF-80-12, (c and d) $Fe(OH)_3$/NF-100-12.

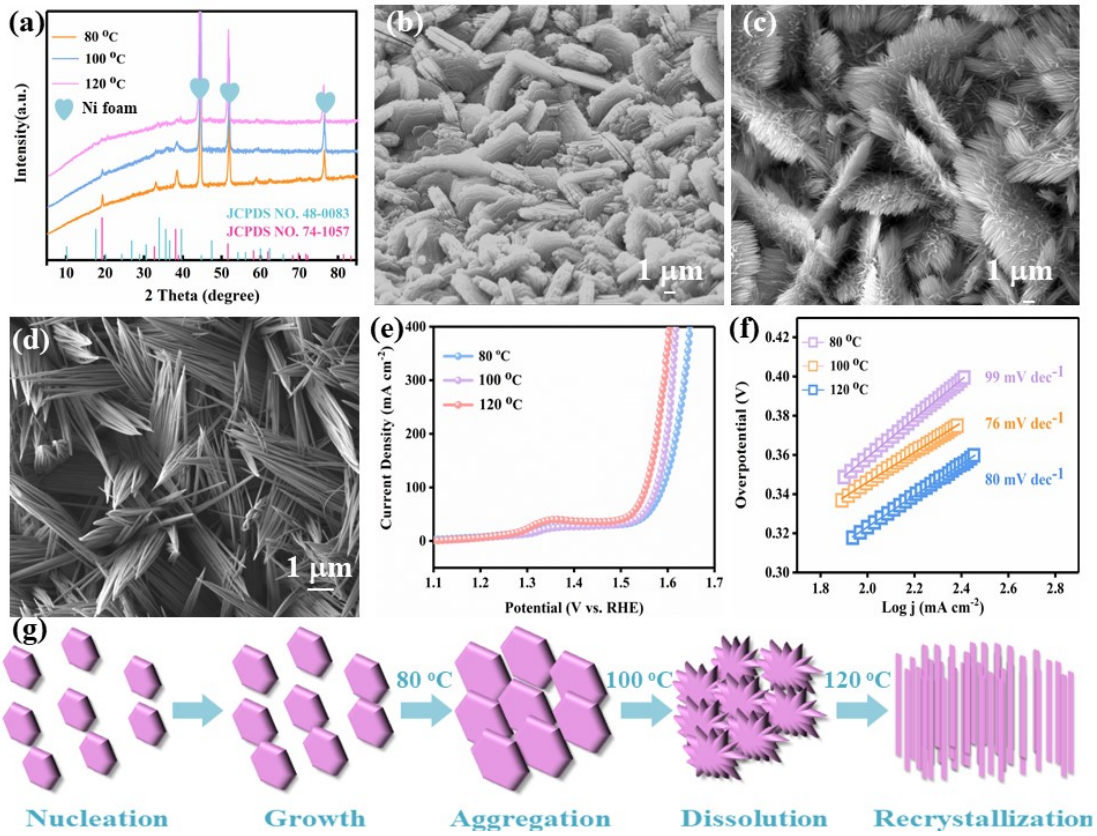


**Fig. S3** (a) XRD patterns for $Co(OH)_2$/NF of different hydrothermal temperatures; SEM image of (b) $Co(OH)_2$/NF-80-12, (c) $Co(OH)_2$/NF-100-12 and (d) $Co(OH)_2$/NF-120-12; (e) LSV curves and (f) Tafel plots of $Co(OH)_2$/NF-x-12 (x=80, 100, 120); (g) the growth process of CCH nanowires.

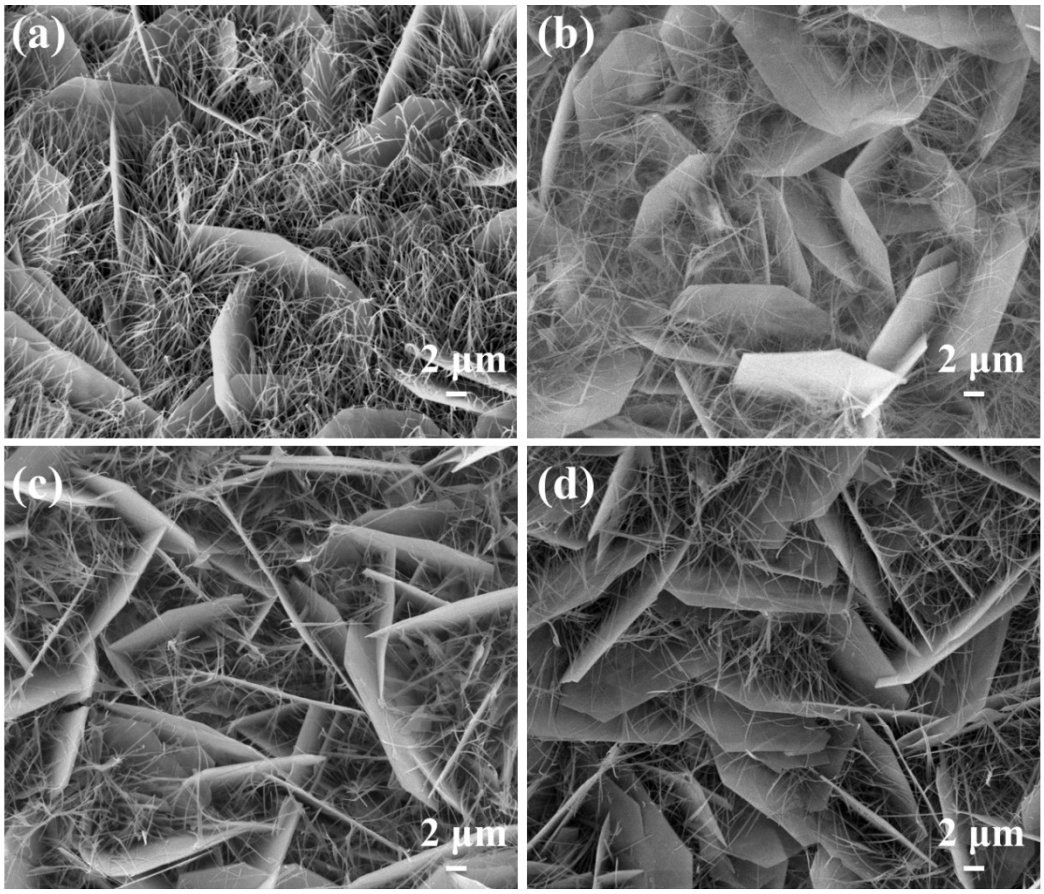


**Fig. S4** SEM image of (a) CoFe-LDH-120-8; (b) CoFe-LDH-120-10; (c) CoFe-LDH-120-12; (d) CoFe-LDH-120-14.

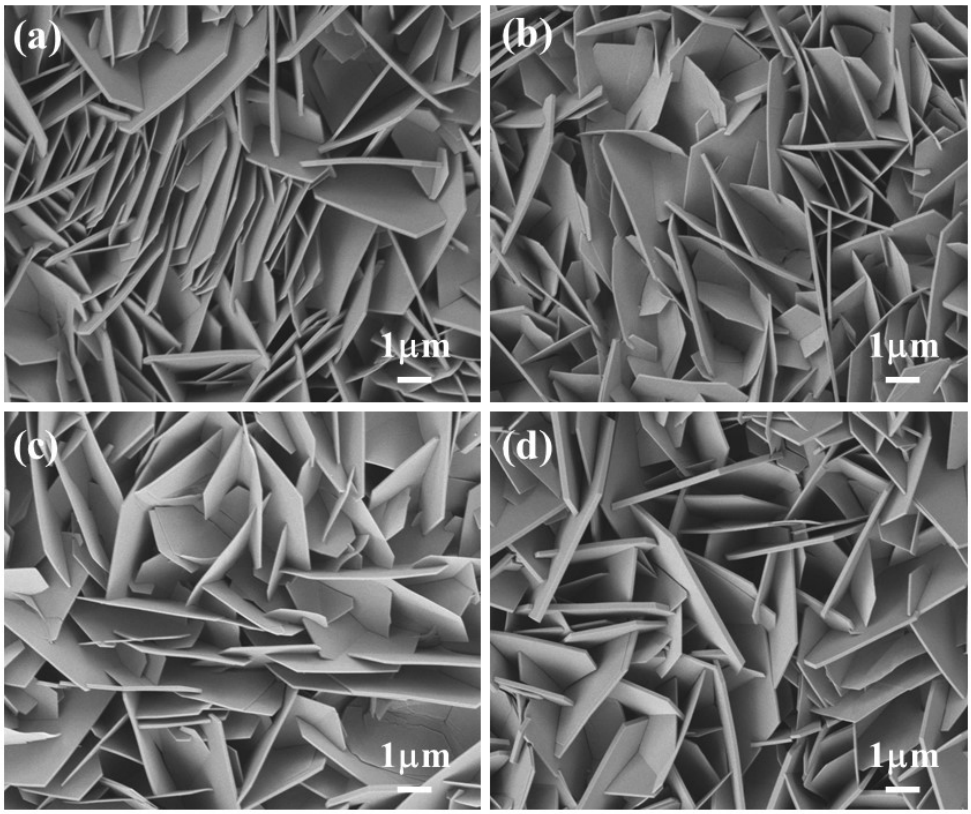


**Fig. S5** SEM image of (a) CoFe-LDH-80-8; (b) CoFe-LDH-80-10; (c) CoFe-LDH-80-12; (d) CoFe-LDH-80-14.

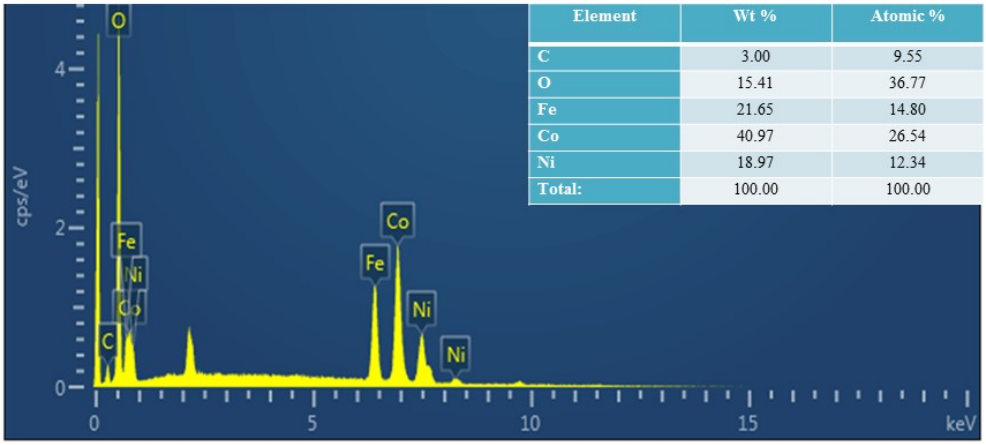


| Element | Wt % | Atomic % |
|---|---|---|
| C | 3.00 | 9.55 |
| O | 15.41 | 36.77 |
| Fe | 21.65 | 14.80 |
| Co | 40.97 | 26.54 |
| Ni | 18.97 | 12.34 |
| Total: | 100.00 | 100.00 |

**Fig. S6** Typical energy-dispersive X-ray spectroscopy (EDS) for CoFe-LDH-120-12.

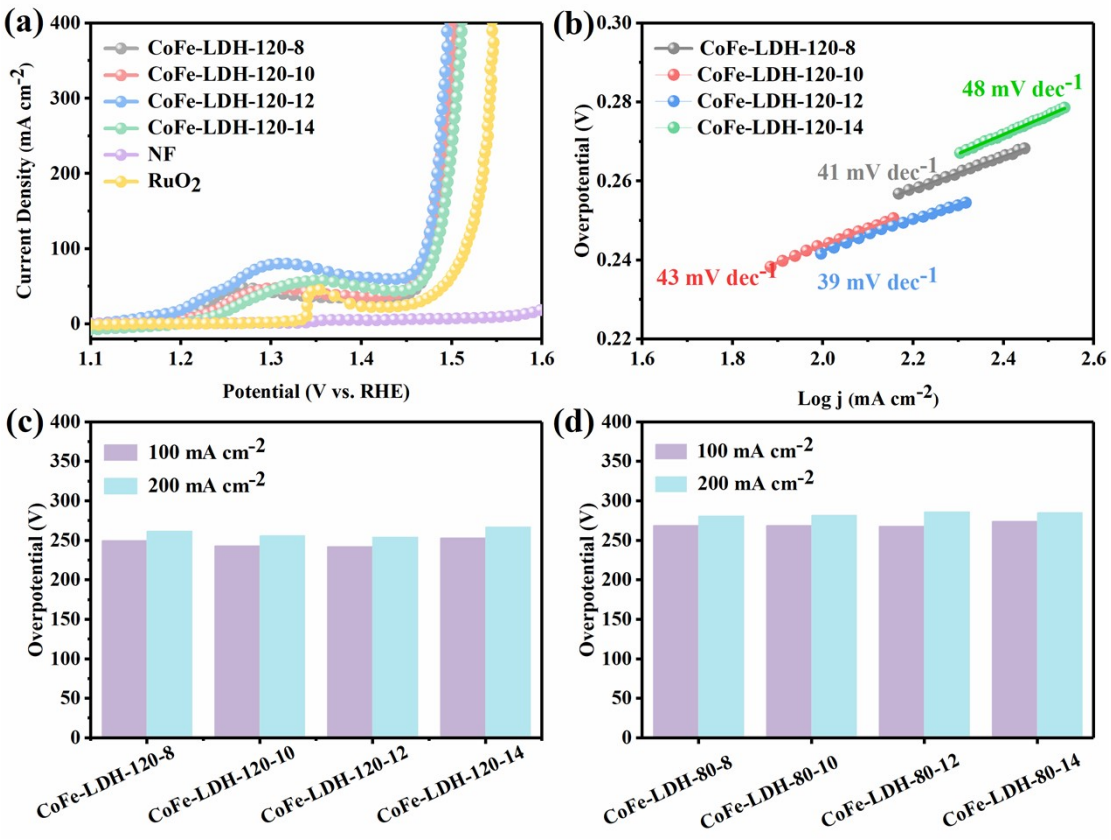


**Fig. S7** (a) LSV curves of CoFe-LDH-120-8, CoFe-LDH-120-10, CoFe-LDH-120-12, CoFe-LDH-120-14, Ni foam (NF) and $RuO_2$ in 1 M KOH solution (scan rate 2mV $s^{-1}$); (b) Tafel plots of the corresponding synthesized catalysts; (c) Overpotential of CoFe-LDH-120-8, CoFe-LDH-120-10, CoFe-LDH-120-12, CoFe-LDH-120-14 at 100 and 200 mA $cm^{-2}$; (d) Overpotentials of CoFe-LDH-80-8, CoFe-LDH-80-10, CoFe-LDH-80-12, CoFe-LDH-80-14 at 100 and 200 mA $cm^{-2}$.

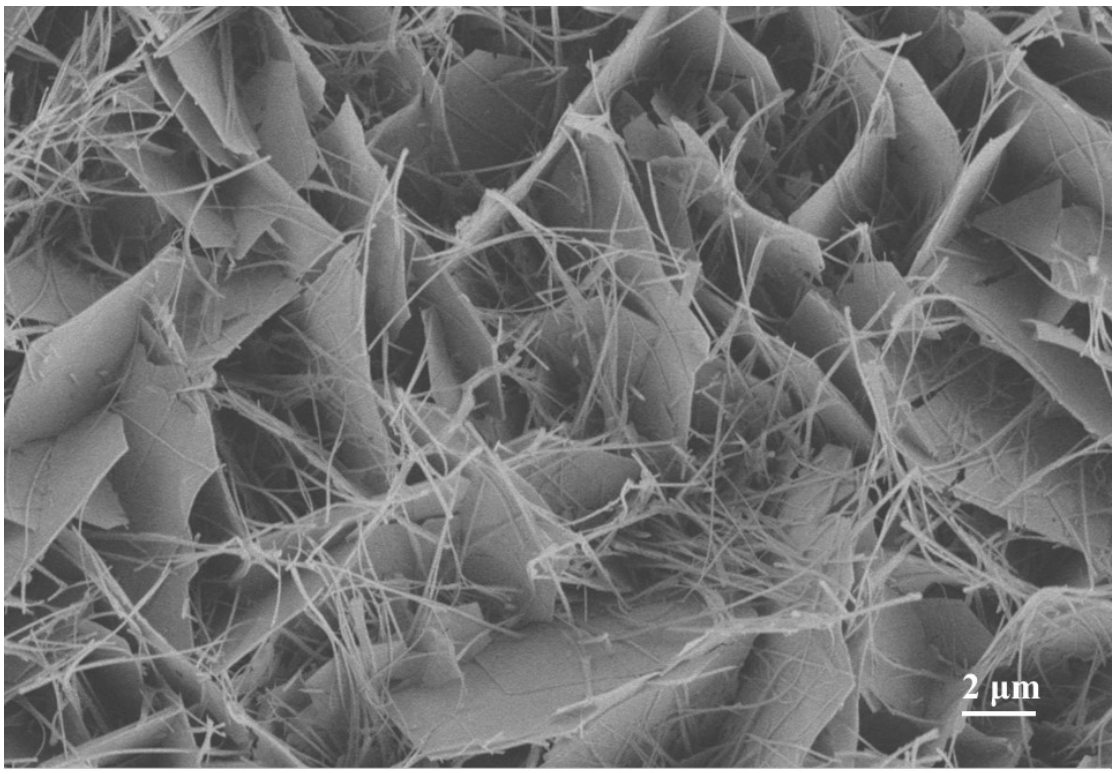


**Fig. S8** SEM image of CoFe-LDH-120 after continuous 97h OER measurement.

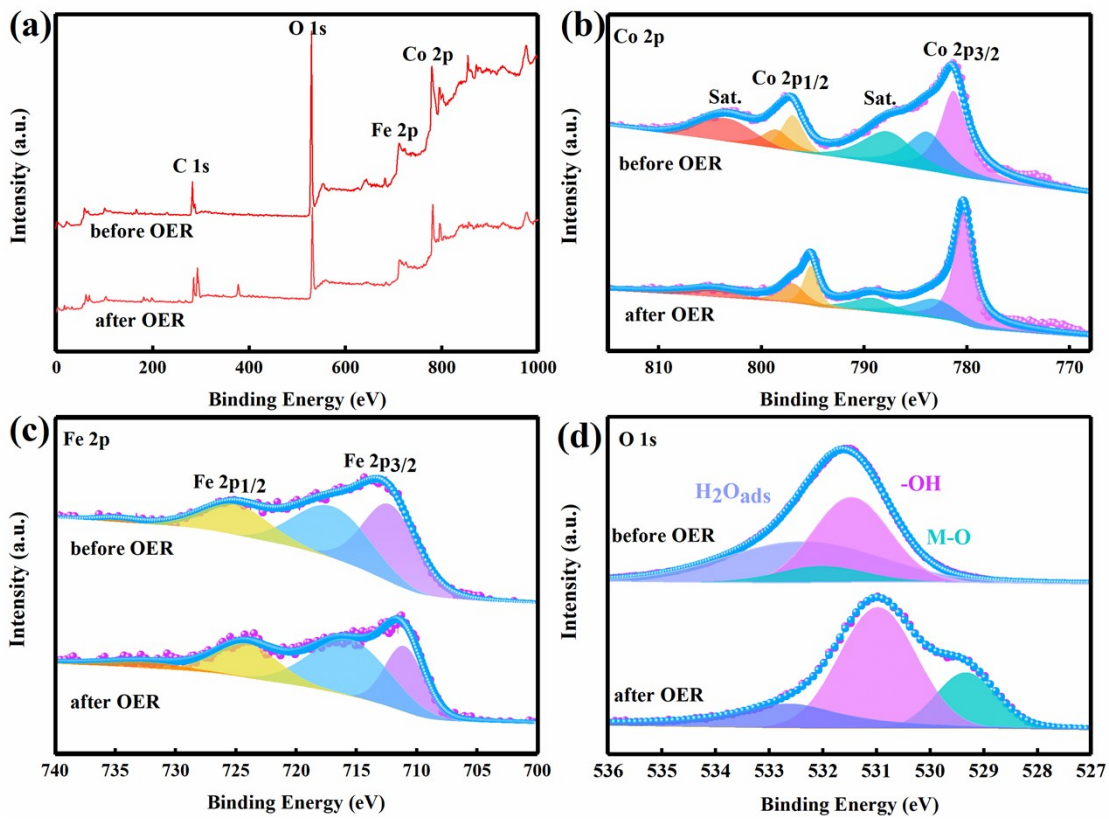


**Fig. S9** XPS full spectrum and XPS spectra of (b) Co 2p, (c) Fe 2p and (d) O 1s performed on CoFe-LDH-120-12 before and after long-term OER electrolysis.

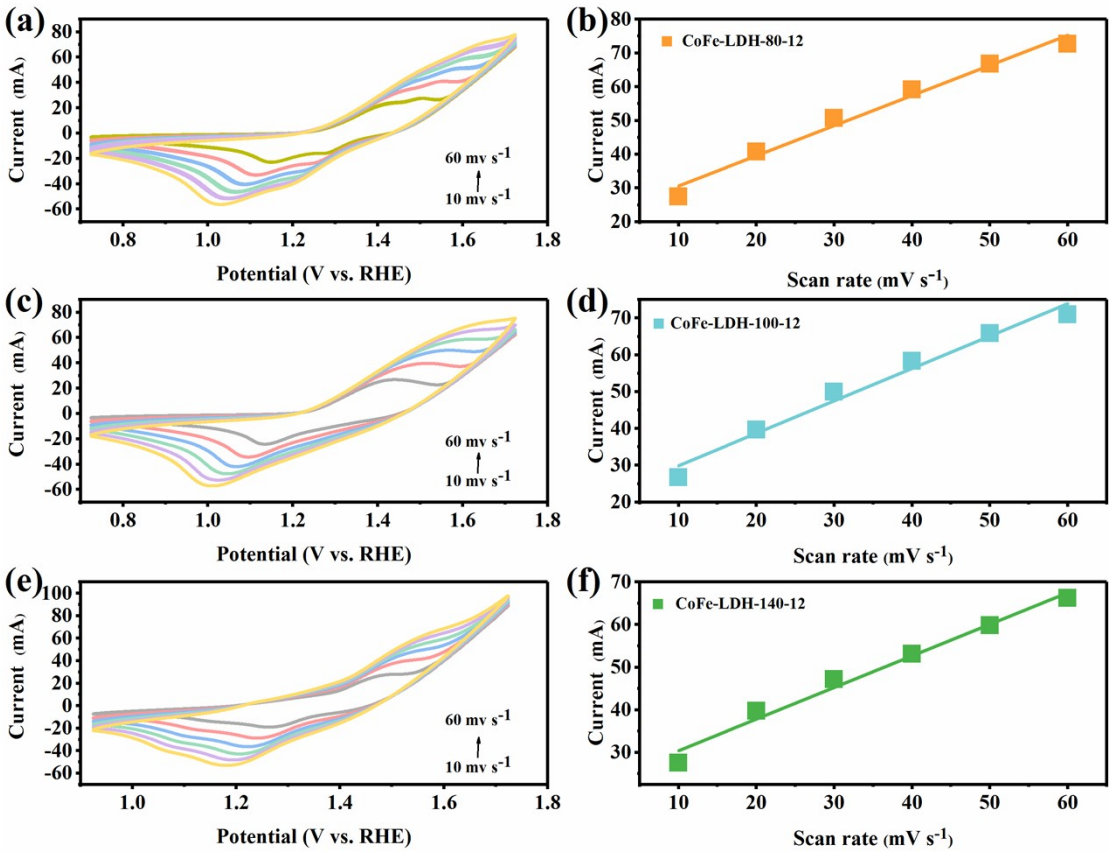


**Fig. S10** The CV curves of different rates of (a) CoFe-LDH-80-12, (c) CoFe-LDH-100-12, (e) CoFe-LDH-140-12; linear relationships of the oxidation peak currents vs. scan rates for (b) CoFe-LDH-80-12, (d) CoFe-LDH-100-12, (f) CoFe-LDH-140-12.

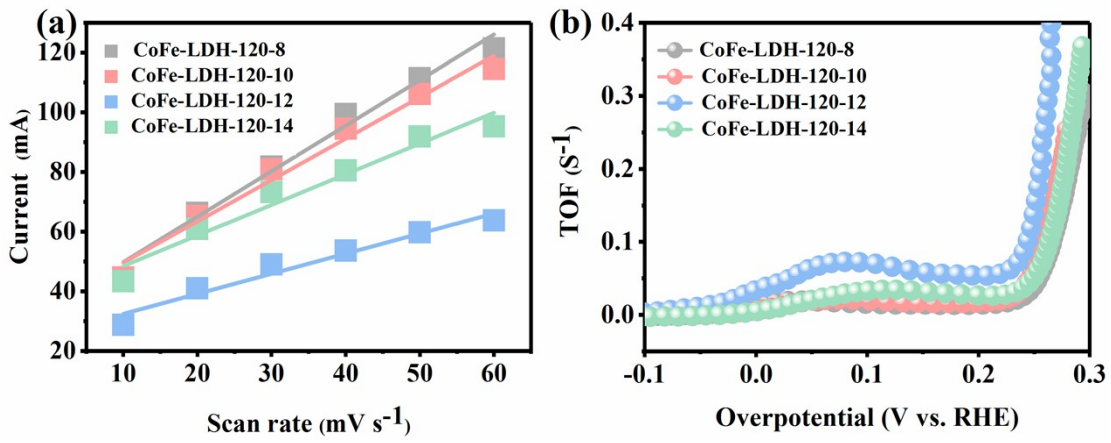


**Fig. S11** (a) Linear relationships of the oxidation peak currents vs. scan rates for CoFe-LDH-120-y (y=8, 10, 12, 14); (b) Turnover frequencies (TOFs) of CoFe-LDH-120- y (y=8, 10, 12, 14).

**Table. S1.** Comparison of the catalytic OER performance between the obtained materials in this work and other various reported LDH-based electrocatalysts in 1 M KOH.

| Catalyst | Electrolyte | $\eta_j$=100 ( mV ) | $\eta_j$=10 ( mV ) | Tafel slope (mV $dec^{-1}$) | Reference |
|---|---|---|---|---|---|
| CoFe-LDH-120-12 | 1 M KOH | 242 | \ | 41 | This Work |
| CoMn-LDH | 1 M KOH | \ | 324 | 43 | [1] |
| NiCoFe-LDH | 1 M KOH | \ | 280 | 34 | [2] |
| Ni-Fe LDH/3D-ErGO | 1 M KOH | \ | 259 | 39 | [3] |
| $IrO_2$@SL-NiFe LDHs | 1 M KOH | \ | 270 | 59 | [4] |
| NiFe LDH@NiCoP/NF | 1 M KOH | \ | 220 | 48.6 | [5] |
| CuO@ZnCo LDH/CF | 1 M KOH | \ | 270 | 100 | [6] |
| Cu@NiFe LDH | 1 M KOH | 281 | 199 | 27.8 | [7] |
| Co@NiFe-LDH | 1 M KOH | \ | 267 | 42 | [8] |
| $Co_{1-x}Fe_x$-LDH | 1 M KOH | 270 | 170 | 36 | [9] |
| CoFe-LDH@Cu foam | 1 M KOH | 300 | 240 | 44.4 | [10] |

| | | | | | |
|---|---|---|---|---|---|
| CoFe-LDH-Ar | 1 M KOH | \ | 266 | 37.85 | [11] |
| NiFe-LDH/NF | 1 M KOH | 297 | \ | 60.8 | [12] |
| $NaBH_4$–NiFe LDH | 1 M KOH | \ | 280 | 56 | [13] |
| NiFeCo-LDH/CF | 1 M KOH | \ | 249 | 42 | [14] |
| NiFe LDH/CB | 1 M KOH | \ | 220 | 35 | [15] |
| NiFe LDH/NiTe | 1 M KOH | 228($\eta_j$=50) | \ | 51.04 | [16] |
| Mn-Co LDH/Graphene | 1 M KOH | \ | 330 | 48 | [17] |
| Ta-NiFe LDH | 1 M KOH | 260($\eta_j$=50) | \ | 58.95 | [18] |
| CoNi LDH/$Ti_3C_2T_x$ | 1 M KOH | 257.4 | \ | 68 | [19] |
| Ni–Fe LDH | 1 M KOH | \ | 260 | 55.6 | [20] |

## Experimental Section

### 1.1 Materials and chemicals

Cobalt nitrate hexahydrate ($Co(NO_3)_2 \cdot 6H_2O$, Sinopharm Chemical Reagent Co., Ltd.), iron(II) sulfate heptahydrate ($FeSO_4 \cdot 7H_2O$ Sinopharm Chemical Reagent Co., Ltd.), urea ($CO(NH_2)_2$, Sinopharm Chemical Reagent Co., Ltd.), ammonia fluoride ($NH_4F$, Sinopharm Chemical Reagent Co., Ltd.), anhydrous ethanol ($CH_3CH_2OH$, Sinopharm Chemical Reagent Co., Ltd.), ruthenium (IV) oxide (Adamas-beta), nafion solution (5%, Alfa-Aesar) were used in this work as received from commercial sources without further purification.

### 1.2 Synthesis of CoFe-LDHs with different hydrothermal conditions on Ni foam (CoFe-LDH-x-y, x=80 $^oC$, 100 $^oC$, 120 $^oC$, 140 $^oC$; y=8 h, 10 h, 12 h, 14 h)

The CoFe-LDH-x-y nanoarrays were prepared by a one-step hydrothermal method. Firstly, a piece of Ni foam (3.5cm×6.5cm) was cleaned in the mix solution of HCl (3M) and deionized water by sonication for 20 min to remove surface impurities, following by washing the NF with deionized water several times till pH=7. In a typical synthesis, $Co(NO_3)_2 \cdot 6H_2O$ (4 mmol), $FeSO_4 \cdot 7H_2O$ (2 mmol), $CO(NH_2)_2$ (10 mmol) and $NH_4F$ (12 mmol) were dissolved in 80 mL deionized water under stirring for 20 min to form a clear solution. Then, the mixture was transferred into a 100 mL Teflon-lined stainless autoclave and a piece of cleaned NF was immersed obliquely into the above solution. The autoclave was sealed and maintained at 120 $^oC$ for 12 h. (named as CoFe-LDH-120-12). After cooling down to room temperature naturally, the material was subsequently rinsed by deionized water and ethanol for three times

with the assistance of ultrasonication, and then dried at 60 °C for 4 h to obtain the catalyst. LDHs with the other hydrothermal temperatures and times were synthesized using the same procedure except controlling temperatures or times.

1.3 Synthesis of cobalt hydroxide on Ni foam ($Co(OH)_2$/NF) with different hydrothermal temperatures ($Co(OH)_2$-x-12, x=80 °C, 100 °C, 120 °C)

$Co(OH)_2$/NF was synthesized by the same procedure except that only 4 mmol cobalt nitrate hexahydrate as metal salt was added.

1.4 Synthesis of iron hydroxide on Ni foam ($Fe(OH)_3$/NF) with different hydrothermal temperatures ($Fe(OH)_3$-x-12, x=80 °C, 100 °C)

$Fe(OH)_3$/NF was synthesized by the same procedure except that only 2 mmol iron(II) sulfate heptahydrate as metal salt was added.

1.5 Preparation of $RuO_2$/NF catalyst

To prepare $RuO_2$/NF catalytic electrode, 22 mg $RuO_2$ and 20 μL 5 wt% nafion solution were dispersed in 1 mL water/ethanol solvent (490 μL ultrapure water and 490 μL ethanol). Then, the mixed solution was treated with ultrasound for 10 h to form uniformly distributed catalyst ink. Then 75 μL of the $RuO_2$ ink (the same loading of 6.6 mg $cm^{-2}$ as CoFe-LDH/NF) was added on NF and dried at air.

1.6 Materials Characterization

Powder X-ray diffraction (XRD) patterns were obtained by a Rigaku D/max-2400 diffractometer with Cu-Kα radiation. The scanning electron microscopy (SEM) images were collected by a Hitachi S-4800 (Chiyoda-ku, Tokyo, Japan) operated at 7 kV. High-resolution transmission electron microscopy (HR-TEM) coupled with

transmission electron microscopy (TEM) were performed by a FEI (TecnaiTM F30, USA) microscope with capabilities for energy-dispersive Xray spectroscopy (EDX, TECNAI G2, USA) operating at 200 KV. X-ray photoelectron spectroscopy (XPS) was also used to characterize chemical bonds of the materials.

1.7 Electrochemical measurements

All OER measurements were carried out with an electrochemical workstation (CHI660E, Shanghai, China) in a three-electrode system in 1 M KOH solution. The CoFe-LDH/NF was used as working electrode, the saturated Hg/HgO was served as reference electrode and the carbon rod was used counter electrode. The linear sweep voltammetry (LSV) polarization curves were analyzed at a scan rate of 2 mV $s^{-1}$ in the potential range from 0 to 1 V. All potentials were calibrated by the following Nernst equation:

$$E_{(RHE)} = E_{(Hg/HgO)} + 0.059pH + 0.098\ V \quad (1)$$

$$\eta_{(overpotential)} = E_{(RHE)} - 1.23\ V \quad (2)$$

In addition, the Tafel slope was acquired with corresponding LSV according to Tafel equation:

$$\eta = b\log j + a \quad (3)$$

Where η is the overpotential, b is the Tafel slope, J is the current density and *a* is the constant at current density of 1 mA $cm^{-2}$. Then a continuous CV of CoFe-LDH for 2000 cycles at a scan rate of 100 mV $s^{-1}$ was measured. The stability of the catalysts was evaluated by chronopotentiometric measurement in 1.0 M KOH electrolyte with the current density at 100 mA $cm^{-2}$ for 97 h.

**References**

1. F. Song and X. Hu, *Journal of the American Chemical Society*, 2014, **136**, 16481-16484.

2. T. Wang, W. Xu and H. Wang, *Electrochimica Acta*, 2017, **257**, 118-127.

3. X. Yu, M. Zhang, W. Yuan and G. Shi, *Journal of Materials Chemistry A*, 2015, **3**, 6921-6928.

4. D. Li, T. Li, G. Hao, W. Guo, S. Chen, G. Liu, J. Li and Q. Zhao, *Chemical Engineering Journal*, 2020, **399**, 125738.

5. H. Zhang, X. Li, A. Hähnel, V. Naumann, C. Lin, S. Azimi, S. L. Schweizer, A. W. Maijenburg and R. B. Wehrspohn, *Advanced Functional Materials*, 2018, **28**, 1706847.

6. T. Wang, X. Zhang, X. Zhu, Q. Liu, S. Lu, A. M. Asiri, Y. Luo and X. Sun, *Nanoscale*, 2020, **12**, 5359-5362.

7. L. Yu, H. Zhou, J. Sun, F. Qin, F. Yu, J. Bao, Y. Yu, S. Chen and Z. Ren, *Energy & Environmental Science*, 2017, **10**, 1820-1827.

8. X. Long, S. Xiao, Z. Wang, X. Zheng and S. Yang, *Chemical Communications*, 2015, **51**, 1120-1123.

9. G. Rajeshkhanna, T. I. Singh, N. H. Kim and J. H. Lee, *ACS Applied Materials & Interfaces*, 2018, **10**, 42453-42468.

10. L. Yu, H. Zhou, J. Sun, F. Qin, D. Luo, L. Xie, F. Yu, J. Bao, Y. Li, Y. Yu, S. Chen and Z. Ren, *Nano Energy*, 2017, **41**, 327-336.

11. Y. Wang, Y. Zhang, Z. Liu, C. Xie, S. Feng, D. Liu, M. Shao and S. Wang,

*Angewandte Chemie International Edition*, 2017, **56**, 5867-5871.

12. M. Salmanion and M. M. Najafpour, *Inorganic Chemistry*, 2021, **60**, 6073-6085.

13. Y. Wang, S. Tao, H. Lin, S. Han, W. Zhong, Y. Xie, J. Hu and S. Yang, *RSC Advances*, 2020, **10**, 33475-33482.

14. Y. Lin, H. Wang, C. K. Peng, L. Bu, C. L. Chiang, K. Tian, Y. Zhao, J. Zhao, Y. G. Lin, J. M. Lee and L. Gao, *Small*, 2020, **16**, 2002426.

15. T. S. Munonde, H. Zheng and P. N. Nomngongo, *Ultrasonics Sonochemistry*, 2019, **59**, 104716.

16. L. Hu, X. Zeng, X. Wei, H. Wang, Y. Wu, W. Gu, L. Shi and C. Zhu, *Applied Catalysis B: Environmental*, 2020, **273**, 119014.

17. J. Bao, J. Xie, F. Lei, Z. Wang, W. Liu, L. Xu, M. Guan, Y. Zhao and H. Li, *Catalysts*, 2018, **8**, 350.

18. X. Wang, Y. Tuo, Y. Zhou, D. Wang, S. Wang and J. Zhang, *Chemical Engineering Journal*, 2021, **403**, 126297.

19. L. Hu, M. Li, X. Wei, H. Wang, Y. Wu, J. Wen, W. Gu and C. Zhu, *Chemical Engineering Journal*, 2020, **398**, 125605.

20. H. Yang, S. Luo, Y. Bao, Y. Luo, J. Jin and J. Ma, *Inorganic Chemistry Frontiers*, 2017, **4**, 1173-1181.